Available online at www.sciencedirect.com

ScienceDirect

International Journal of Mass Spectrometry 261 (2007) 57–67

International Journal of Mass Spectrometry

www.elsevier.com/locate/ijms

A density functional study of the structures and energies of $C_nN_5^-$ ($n = 1–13$) clusters

M.D. Chen [a,*], J.W. Liu [a,1], L. Dang [a], Q.E. Zhang [a], C.T. Au [b]

[a] *State Key Laboratory of Physical Chemistry of Solid Surfaces, Department of Chemistry, College of Chemistry and Chemical Engineering, Center for Theoretical Chemistry, Xiamen University, Xiamen 361005, People's Republic of China*

[b] *Department of Chemistry, Hong Kong Baptist University, Kowloon Tong, Hong Kong, People's Republic of China*

Received 24 February 2006; received in revised form 25 July 2006; accepted 25 July 2006

Available online 26 September 2006

Abstract

We designed numerous models of $C_nN_5^-$ ($n = 1–13$) using molecular graphics software. Geometry optimization and calculation of vibration frequency were carried out by means of the B3LYP density functional approach. After comparison of structure stability, we found that the ground-state structure of CN_5^- shows a N_4CN chain configuration whereas those of $C_nN_5^-$ ($n = 2–13$) contain a planar pentagonal ring compose of nitrogen and carbon atoms when $n \leq 8$, and of carbon atoms only when $9 \leq n$. For odd-*n* ground-state isomers with $1 < n \leq 9$, one carbon atom of the ring is bonded to a nitrogen atom and the other carbon atom(s) are bonded to a cyano (–CN) group. When *n* is even and with $2 \leq n \leq 10$, all the carbon atom(s) within the ring are bonded to a cyano group. When $n = 11–13$, one of the carbon atoms of the ring is bonded to a straight NC_2–, NC_3– and NC_4– chain, respectively, while the other carbon atoms of the ring are each bonded to a cyano group. The NC_2– and NC_4– chains show cumulenic-like structures whereas the NC_3– chain shows polyacetylene-like structure. According to total energies, the $C_nN_5^-$ with even *n* are more stable than those with odd *n*, matching the peak patterns observed in the mass spectra of $C_nN_5^-$. The trend of such odd/even alternation can be explained based on concepts of bonding characters, energy differences, electron affinities, and incremental binding energies.

Keywords: Binary cluster anion; $C_nN_5^-$; Nitrogen-doped cluster; Density functional study

1. Introduction

The discovery of strange carbon compounds and clusters has opened up research fields of new magnitude. Carbon clusters containing nitrogen have been detected in celestial bodies [1–3], and recent results of experimental and theoretical investigations on binary clusters prompted further enthusiasm. In the search of new materials, scientists have worked on nitrides of various types. It was reported that carbon/nitrogen binary clusters can be generated by means of unconventional methods such as laser ablation [4–6]. According to the theoretical prediction of Niu et al., crystalline β-C_3N_4 is comparable to diamond in hardness [4]. To understand the nature of these cluster-assembled substances that differ greatly in properties, scientists have been conducting examinations on the geometric structures and ground-state electronics of the materials. Recently, there have been reports on the theoretical investigations of nitrogen-doped carbon clusters. Using the HF method, Wang et al. carried out calculations on linear C_nN^- and showed that the odd-*n* isomers are much more stable than the even-*n* ones, in good agreement with the experimental results [7]. Zhan and Iwata reported the ground states of C_nN^- ($n = 1–13$) after conducting a series of *ab initio* calculations [8]. Pascoli and Lavendy described the linear structures of C_nN^- ($n = 1–7$) based on the results of density functional calculations and reported that the ground-state isomers are linear in structure [9]. Tittle et al. analyzed C_5N_2 clusters by adopting the density functional method [10]. Armstrong et al. did calculations on the ionization energies of CN_2 isomers at the G1 and G2 levels [11]. Chuchev and Belbruno conducted B3LYP density functional calculations on structures of C_6N, C_6N_2, and C_nN_2 and made prediction on the most stable isomers [12–14]. BelBruno investigated the structures and energies of C_3N_4 by *ab initio* calculation [15], and those of carbon/nitrogen clusters with up to 12 atoms by density functional calculations [16].

---

[*] Corresponding author. Tel.: +86 592 2182332; fax: +86 592 2184708.
E-mail address: mdchen@xmu.edu.cn (M.D. Chen).

[1] Present address: Department of Chemistry, The Chinese University of Hong Kong, Shatin, Hong Kong, People's Republic of China.

1387-3806/$ – see front matter © 2006 Elsevier B.V. All rights reserved.
doi:10.1016/j.ijms.2006.07.018

Jiang et al. carried out density functional study on structures and stabilities of $C_nN_2^-$ ($n = 1$–14) ions [17]. Tang et al. studied the structures and energies of cyclic $C_{2n}N_5^-$ ($n = 1$–6) clusters by means of B3LYP/6-31G* calculations [18]. Recently, we performed density functional studies on the structures and energies of $C_nN_3^-$ ($n = 1$–8) [19], and Lord et al. investigated the structures and energetics of the pentacyanocyclopentadienyl (PCCP) system by means of DFT methods [20].

Despite the various works that have been done on nitrogen-doped carbon clusters, our understanding of these materials is still limited. In the time-of-flight mass spectra of $C_nN_m^-$ [5], $C_nN_5^-$ exhibited even/odd alternation in signal intensity: signal intensities of anionic clusters with even n are generally higher than those with odd n. To explore these experimental observations theoretically, we designed numerous structural models of $C_nN_5^-$ ($n = 1$–13), and performed geometry optimization and calculations on vibration frequencies by means of the B3LYP density functional method. The stabilities, geometry structures, bonding characters, energy differences, electron affinities, and incremental binding energies of the clusters have been investigated. Based on the results, we provide insights into why the $C_nN_5^-$ ($n = 1$–13) isomers with even n are more stable than those with odd n.

2. Computational methods

Devices for molecular graphics, molecular mechanics, and quantum chemistry were used for the investigation. First, a three-dimensional model of a cluster was designed using HyperChem for Windows [21] and Desktop Molecular Modeler for Windows [22] on a PC/Pentium IV computer. Then, the model was optimized by MM+ molecular mechanics and semi-empirical PM3 quantum chemistry. Last, geometry optimization and calculations of vibration frequencies were conducted using the B3LYP density functional method of Gaussian 98 package [23] with 6-311G* basis sets, i.e., Becke's three-parameter non-local exchange functional with the correlation functional of Lee et al. [24–26]. The single point energy calculations following the optimizations were performed by using the larger 6-311+G* basis set, including diffuse functions (i.e., B3LYP/6-311+G*//B3LYP/6-311G*) [27]. All energies were calculated with zero point energy (ZPE) correction [28]. The optimized models were again displayed using HyperChem for Windows. The data of partial charges and bond orders were analyzed with Gaussian Natural Bond Orbital (NBO). All of the calculations were carried out on the servers of SGI.

3. Results and discussion

3.1. Geometry and energy

At the beginning of the study, nothing was known other than the $C_nN_5^-$ ($n = 1$–13) formula. The assumption of a reasonable geometrical structure was the initial step for the optimization of the new clusters. First we examined a large number of possible models which are reasonable in chemical understandings, among which are linear, cyclic, and bicyclic, as well as three-dimensional structures. After a number of trial optimizations, the results are summarized and models with imaginary vibration frequencies and/or of higher energies are discarded; those configurations are not considered as initial models. Shown in Figs. 1–13 are the isomers corresponding to local minima of $C_nN_5^-$ ($n = 1$–13) with both singlet and triplet forms optimized. We only include here the stable isomers with real vibration frequencies and those with imaginary frequencies and of higher energies are excluded. In the case of triplet-state $C_nN_5^-$

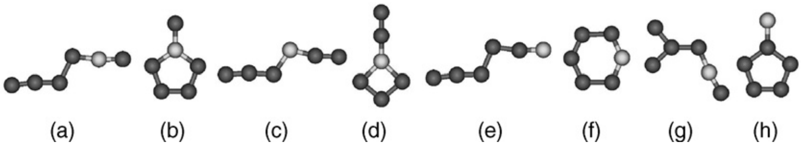

Fig. 1. Eight isomers of CN_5^-.

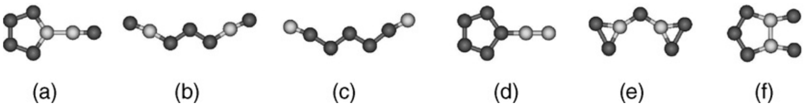

Fig. 2. Six isomers of $C_2N_5^-$.

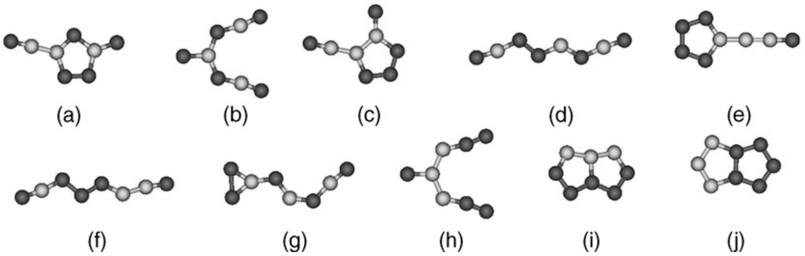

Fig. 3. Ten isomers of $C_3N_5^-$.

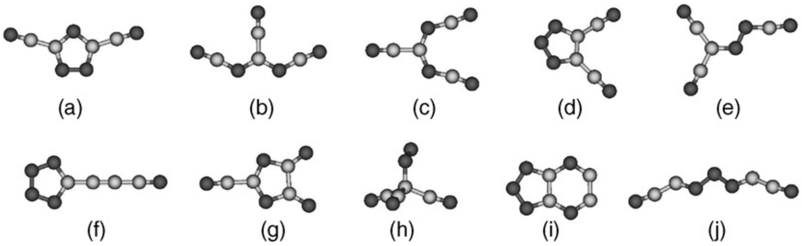

Fig. 4. Ten isomers of $C_4N_5^-$.

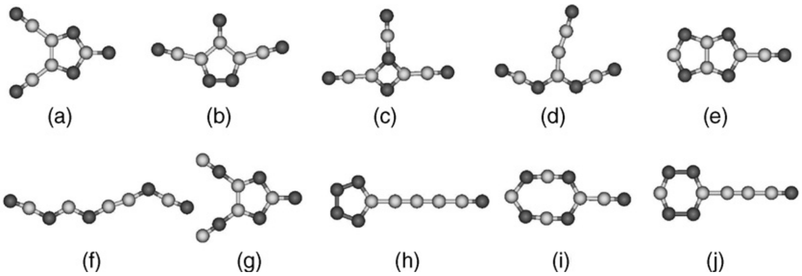

Fig. 5. Ten isomers of $C_5N_5^-$.

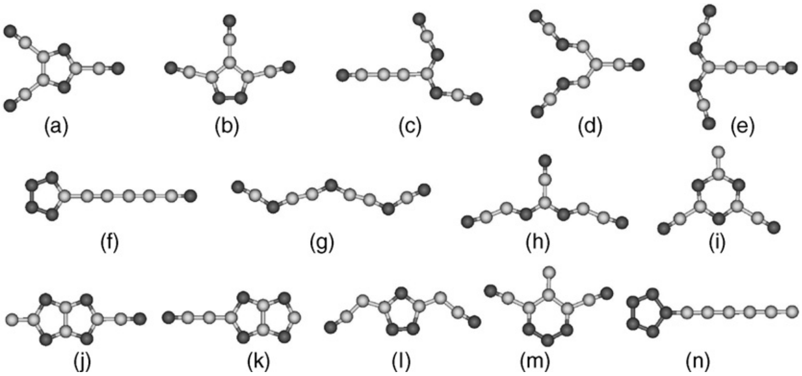

Fig. 6. Fourteen isomers of $C_6N_5^-$.

($n = 1$–13) isomers, spin contamination $\langle S^2 \rangle$ value (before annihilation of the contaminants) is between 2.01 and 2.08, i.e., within 4% of the expected value of 2.0; such slight deviation should not have a large effect on our results. In each figure, the models are arranged in the order of ascending total energy; light-gray balls represent carbon atoms and dark-gray ones denote nitrogen atoms. Many of the models depicted in this paper have never been reported before. The calculated structures are presented in Figs. 1–13.

Listed in Table 1 are the symmetries, total energies, electronic states, and relative energies of the $C_nN_5^-$ ($n = 1$–13) structures shown in Figs. 1–13. Model 1a shows a chain configuration with a terminal –CN unit. Model 1b (7.22 kcal/mol higher than Model 1a in energy) is a structure with a nitrogen atom bonded

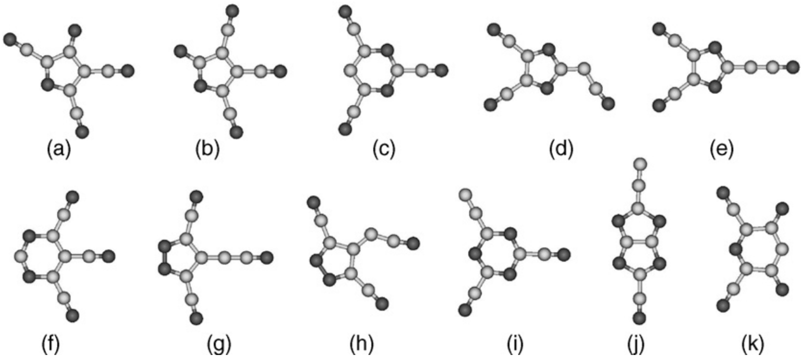

Fig. 7. Eleven isomers of $C_7N_5^-$.

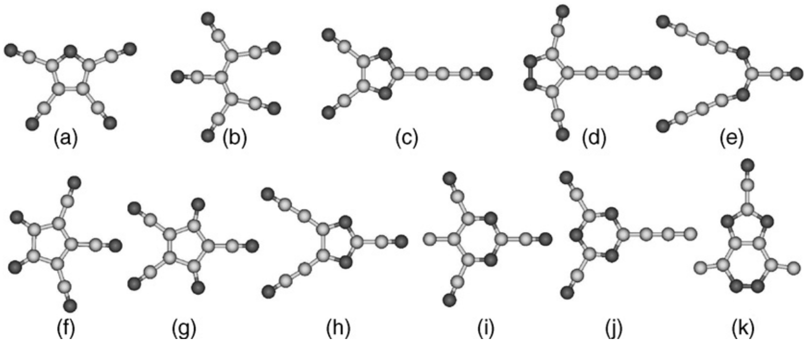

Fig. 8. Eleven isomers of $C_8N_5^-$.

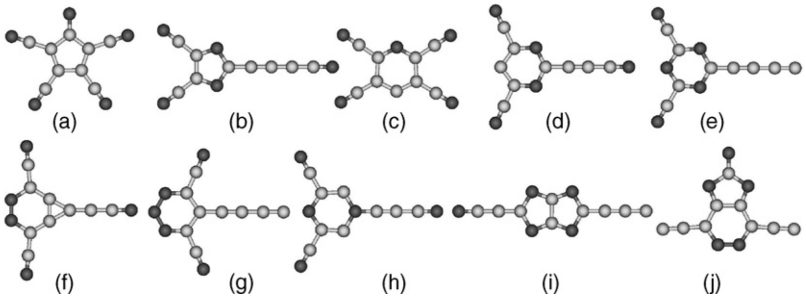

Fig. 9. Ten isomers of $C_9N_5^-$.

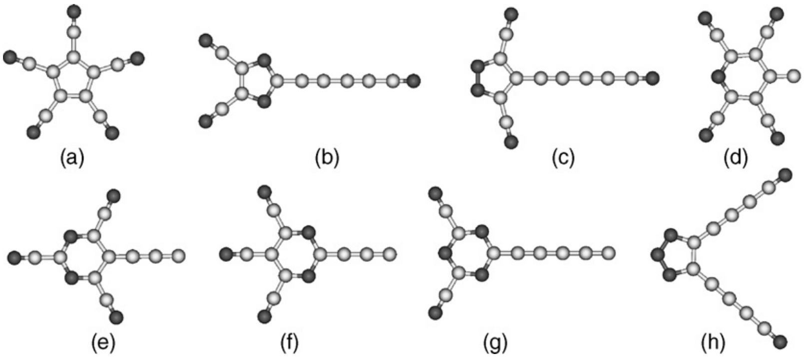

Fig. 10. Eight isomers of $C_{10}N_5^-$.

to the carbon atom of a pentagonal N_4C ring. The data so far indicate that with $n = 2$–8, the $C_nN_5^-$ anions of lowest energy contain a planar pentagonal ring composes of nitrogen and carbon atoms, and each carbon atom in the ring is bonded to either a cyano (–CN) group or a nitrogen atom. Model 2a displays a structure with a cyano group bonded to the carbon atom of the CN_4 ring. Model 3a is a $C_3N_5^-$ structure with the two carbon atoms of the C_2N_3 ring bonded to a nitrogen atom and a cyano

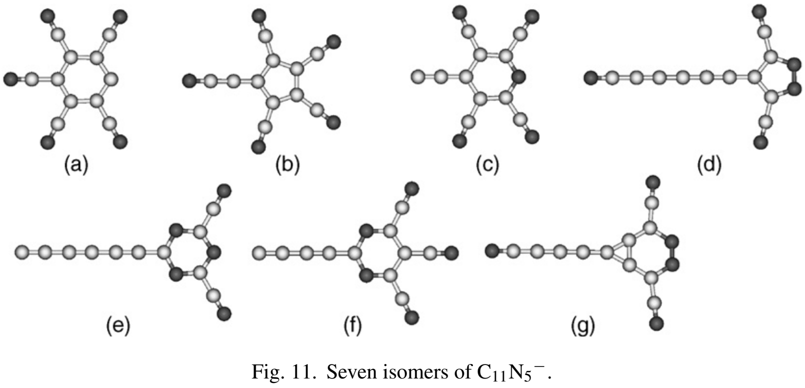

Fig. 11. Seven isomers of $C_{11}N_5^-$.

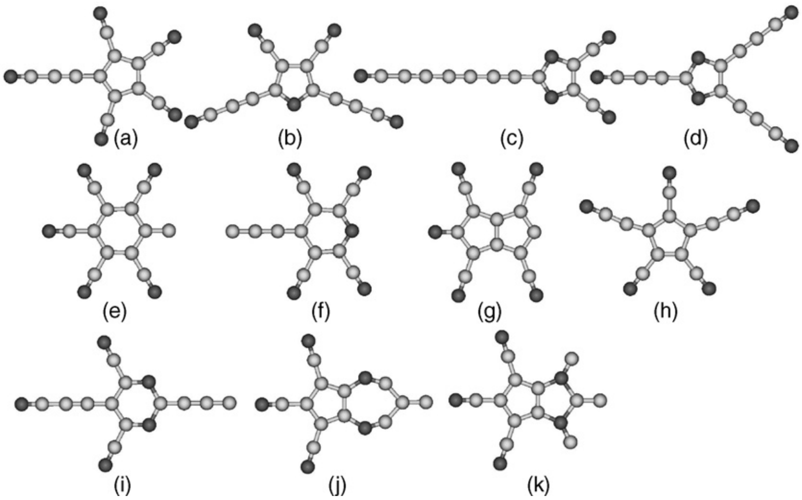

Fig. 12. Eleven isomers of $C_{12}N_5^-$.

group, respectively. Model 4a is with each of the carbon atoms of the C_2N_3 ring bonded to a cyano group, whereas Model 5a is with one carbon atom of the C_3N_2 ring bonded to a nitrogen atom and each of the other two carbon atoms bonded to a cyano group. Model 6a is similar to Model 5a in structure, only that each of the three carbon atoms of the C_3N_2 ring is decorated with a cyano group. Model 7a is with the carbon atoms of the C_4N ring bonded to a nitrogen atom and three cyano groups, respectively. Model 8a is with each of the four carbon atoms of the C_4N ring bonded to a cyano group. With $n = 9–13$, the ring of the most stable isomers is composed of carbon atoms only. Model 9a is with one carbon atom of the C_5 ring bonded to a nitrogen atom and each of the other carbon atoms bonded to a cyano group. Model 10a is with each of the carbon atoms of the C_5 ring bonded to a cyano group. As for $C_{11}N_5^-$, Model 11a shows a planar C_6 ring with five of the carbon atoms bonded to a cyano group, whereas Model 11b shows a C_5 ring with four of the carbon atoms bonded to a cyano group and the fifth carbon atom bonded to a NC_2– chain. Model 11b is the second most stable; it is beat by Model 11a by 3.26 kcal/mol. In view of such a small difference in relative energy, we consider that Model 11b is also a candidate of ground-state $C_{11}N_5^-$ and have it adopted in Fig. 14. In Models 12a and 13a, the C_5 ring has four carbon atoms bonded to a cyano group and the fifth carbon atom decorated with a NC_3– and NC_4– chain, respectively. Tang et al. investigated the structures and energies of cyclic $C_{2n}N_5^-$ ($n = 1–6$) clusters by means of B3LYP/6-31G* calculations. Our results of ground-state $C_nN_5^-$ with $n = 2, 4, 6, 8, 10, 12$ are in good agreement with the results of Tang et al. [18].

In the case of having isomers close in energy, the methods adopted for theoretical calculation could have an effect on the ordering of energy. In order to confirm that it is not the case in our studies, we performed CCSD(T)/6-311G* computation on CN_5^- as well; the energies for 1a, 1b, 1c, 1d, 1e, 1f, 1g, and 1h are −311.0913, −311.0879, −311.0373, −311.0244, −311.0204, −311.0120, −311.0044, and −311.9890 a.u., respectively. The energy trend is the same as that obtained in B3LYP/6-311+G* calculations.

After the study of a great number of models, including those of Figs. 1–13, it is apparent that "having a nitrogen atom at a terminal position" is preferred for stable clusters regardless of geometry (whether it is branch, chain or cyclic), and such configuration is crucial to the stability of clusters. The relative energy of the isomers for a particular cluster increases as the number of terminal nitrogen atoms decreases. For the clusters with a small number of carbon atoms (i.e., $1 < n < 9$), the pentagonal rings are composed of nitrogen and carbon atoms are popular. An isomer with an N–N bond inside its structure is generally poor in stability. For example, the $C_nN_5^-$ ($n = 2–8$) structures

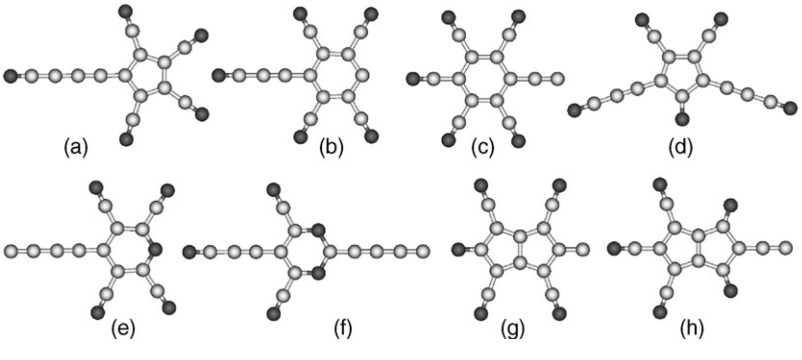

Fig. 13. Eight isomers of $C_{13}N_5^-$.

Table 1
Symmetries, electronic states, total energies (a.u.), and relative energies (kcal/mol) of $C_nN_5^-$ (n = 1–13) isomers

Figure	Cluster	Symmetry	State	Total energy	Relative energy
Fig. 1a	CN_5^-	C_s	$^1A'$	−311.8591	0.00
Fig. 1b	CN_5^-	C_{2v}	$^3A_2$	−311.8476	7.22
Fig. 1c	CN_5^-	C_s	$^1A'$	−311.8093	31.25
Fig. 1d	CN_5^-	C_s	$^1A'$	−311.7916	42.36
Fig. 1e	CN_5^-	C_s	$^1A'$	−311.7882	44.49
Fig. 1f	CN_5^-	C_{2v}	$^3A_2$	−311.7721	54.59
Fig. 1g	CN_5^-	C_s	$^1A'$	−311.7677	57.35
Fig. 1h	CN_5^-	C_{2v}	$^3A_2$	−311.7490	69.09
Fig. 2a	$C_2N_5^-$	C_{2v}	$^1A_1$	−350.0431	0.00
Fig. 2b	$C_2N_5^-$	C_{2v}	$^1A_1$	−350.0181	15.69
Fig. 2c	$C_2N_5^-$	C_{2v}	$^1A_1$	−349.8921	94.75
Fig. 2d	$C_2N_5^-$	C_{2v}	$^1A_1$	−349.8860	98.58
Fig. 2e	$C_2N_5^-$	C_{2v}	$^3B_2$	−349.8838	99.96
Fig. 2f	$C_2N_5^-$	C_{2v}	$^1A_1$	−349.8427	125.75
Fig. 3a	$C_3N_5^-$	C_s	$^3A''$	−388.0975	0.00
Fig. 3b	$C_3N_5^-$	C_{2v}	$^3A_2$	−388.0890	5.33
Fig. 3c	$C_3N_5^-$	C_s	$^3A''$	−388.0798	11.11
Fig. 3d	$C_3N_5^-$	C_s	$^3A''$	−388.0754	13.87
Fig. 3e	$C_3N_5^-$	C_{2v}	$^3A_2$	−388.0593	23.97
Fig. 3f	$C_3N_5^-$	C_s	$^3A''$	−388.0490	30.43
Fig. 3g	$C_3N_5^-$	C_s	$^3A''$	−388.0303	42.16
Fig. 3h	$C_3N_5^-$	C_{2v}	$^3A_2$	−387.9449	95.76
Fig. 3i	$C_3N_5^-$	C_{2v}	$^1A_1$	−387.8594	149.41
Fig. 3j	$C_3N_5^-$	C_s	$^3A''$	−387.8454	158.20
Fig. 4a	$C_4N_5^-$	C_{2v}	$^1A_1$	−426.2911	0.00
Fig. 4b	$C_4N_5^-$	C_s	$^1A'$	−426.2859	3.26
Fig. 4c	$C_4N_5^-$	C_{2v}	$^1A_1$	−426.2851	3.77
Fig. 4d	$C_4N_5^-$	C_{2v}	$^1A_1$	−426.2706	12.86
Fig. 4e	$C_4N_5^-$	C_s	$^1A'$	−426.2514	24.91
Fig. 4f	$C_4N_5^-$	C_{2v}	$^1A_1$	−426.2098	51.02
Fig. 4g	$C_4N_5^-$	C_{2v}	$^3B_2$	−426.1780	70.97
Fig. 4h	$C_4N_5^-$	C_s	$^3A''$	−426.1423	93.37
Fig. 4i	$C_4N_5^-$	C_{2v}	$^3B_2$	−426.1172	109.12
Fig. 4j	$C_4N_5^-$	C_{2v}	$^3B_2$	−426.1086	114.52
Fig. 5a	$C_5N_5^-$	C_{2v}	$^3A_2$	−464.3344	0.00
Fig. 5b	$C_5N_5^-$	C_{2v}	$^3A_2$	−464.3122	13.93
Fig. 5c	$C_5N_5^-$	C_s	$^1A'$	−464.3106	14.93
Fig. 5d	$C_5N_5^-$	C_s	$^3A''$	−464.2982	22.72
Fig. 5e	$C_5N_5^-$	C_2	^3B	−464.2816	33.13
Fig. 5f	$C_5N_5^-$	C_s	$^3A''$	−464.2701	40.35
Fig. 5g	$C_5N_5^-$	C_{2v}	$^3A_2$	−464.2622	45.31
Fig. 5h	$C_5N_5^-$	C_{2v}	$^3A_2$	−464.2498	53.09
Fig. 5i	$C_5N_5^-$	C_{2v}	$^1A_1$	−464.2261	67.96
Fig. 5j	$C_5N_5^-$	C_s	$^3A''$	−464.1878	91.99
Fig. 6a	$C_6N_5^-$	C_{2v}	$^1A_1$	−502.5266	0.00
Fig. 6b	$C_6N_5^-$	C_{2v}	$^1A_1$	−502.5006	16.32
Fig. 6c	$C_6N_5^-$	C_s	$^1A'$	−502.4526	46.44
Fig. 6d	$C_6N_5^-$	C_{2v}	$^1A_1$	−502.3948	82.71
Fig. 6e	$C_6N_5^-$	C_{2v}	$^3A'$	−502.3829	90.17
Fig. 6f	$C_6N_5^-$	C_{2v}	$^1A_1$	−502.3802	91.87
Fig. 6g	$C_6N_5^-$	C_s	$^1A'$	−502.3744	95.51
Fig. 6h	$C_6N_5^-$	C_{2v}	$^3B_2$	−502.3667	100.34
Fig. 6i	$C_6N_5^-$	C_{2v}	$^1A_1$	−502.3525	109.25
Fig. 6j	$C_6N_5^-$	C_{2v}	$^1A_1$	−502.3437	114.77
Fig. 6k	$C_6N_5^-$	C_{2v}	$^3B_2$	−502.3298	123.49
Fig. 6l	$C_6N_5^-$	C_{2v}	$^1A_1$	−502.3160	132.15
Fig. 6m	$C_6N_5^-$	Cs	$^3A''$	−502.2921	147.15
Fig. 6n	$C_6N_5^-$	C_{2v}	$^3A_1$	−502.1636	227.79
Fig. 7a	$C_7N_5^-$	C_s	$^3A''$	−540.5519	0.00
Fig. 7b	$C_7N_5^-$	C_s	$^3A''$	−540.5509	0.63
Fig. 7c	$C_7N_5^-$	C_{2v}	$^1A_1$	−540.5508	0.69
Fig. 7d	$C_7N_5^-$	C_1		−540.5439	5.02
Fig. 7e	$C_7N_5^-$	C_{2v}	$^3A_2$	−540.5420	6.21
Fig. 7f	$C_7N_5^-$	C_{2v}	$^3A_2$	−540.5202	19.89
Fig. 7g	$C_7N_5^-$	C_{2v}	$^3A_2$	−540.5182	21.15
Fig. 7h	$C_7N_5^-$	C_s	$^1A'$	−540.5179	21.34
Fig. 7i	$C_7N_5^-$	C_s	$^1A'$	−540.5005	32.25
Fig. 7j	$C_7N_5^-$	C_s	$^1A'$	−540.4543	61.24
Fig. 7k	$C_7N_5^-$	C_{2v}	$^3A_2$	−540.3886	102.47
Fig. 8a	$C_8N_5^-$	C_{2v}	$^1A_1$	−578.7388	0.00
Fig. 8b	$C_8N_5^-$	C_{2v}	$^1A_1$	−578.7013	23.53
Fig. 8c	$C_8N_5^-$	C_{2v}	$^1A_1$	−578.6916	29.62
Fig. 8d	$C_8N_5^-$	C_{2v}	$^1A_1$	−578.6663	45.49
Fig. 8e	$C_8N_5^-$	C_{2v}	$^1A_1$	−578.6272	70.03
Fig. 8f	$C_8N_5^-$	C_{2v}	$^3B_2$	−578.6037	84.78
Fig. 8g	$C_8N_5^-$	C_{2v}	$^3B_2$	−578.5939	90.93
Fig. 8h	$C_8N_5^-$	C_{2v}	$^3B_2$	−578.5732	103.92
Fig. 8i	$C_8N_5^-$	C_{2v}	$^3A_2$	−578.5631	110.25
Fig. 8j	$C_8N_5^-$	C_{2v}	$^1A_1$	−578.5459	121.05
Fig. 8k	$C_8N_5^-$	C_{2v}	$^1A_1$	−578.4118	205.20
Fig. 9a	$C_9N_5^-$	C_{2v}	$^3A_2$	−616.7677	0.00
Fig. 9b	$C_9N_5^-$	C_{2v}	$^3A_2$	−616.7303	23.44
Fig. 9c	$C_9N_5^-$	C_{2v}	$^3A_2$	−616.7288	24.42
Fig. 9d	$C_9N_5^-$	C_{2v}	$^1A_1$	−616.7136	33.91
Fig. 9e	$C_9N_5^-$	C_{2v}	$^1A_1$	−616.6724	59.77
Fig. 9f	$C_9N_5^-$	C_{2v}	$^3A_2$	−616.6184	80.78
Fig. 9g	$C_9N_5^-$	C_{2v}	$^1A_1$	−616.6168	81.84
Fig. 9h	$C_9N_5^-$	C_{2v}	$^3A_2$	−616.6013	91.53
Fig. 9i	$C_9N_5^-$	C_{2v}	$^3A_2$	−616.5523	122.28
Fig. 9j	$C_9N_5^-$	C_{2v}	$^3B_1$	−616.4499	186.55
Fig. 10a	$C_{10}N_5^-$	C_{2v}	$^1A_1$	−654.9527	0.00
Fig. 10b	$C_{10}N_5^-$	C_{2v}	$^1A_1$	−654.8599	58.22
Fig. 10c	$C_{10}N_5^-$	C_{2v}	$^3B_2$	−654.8341	74.422
Fig. 10d	$C_{10}N_5^-$	C_{2v}	$^1A_1$	−654.7852	105.21
Fig. 10e	$C_{10}N_5^-$	C_{2v}	$^1A_1$	−654.7579	122.21
Fig. 10f	$C_{10}N_5^-$	C_{2v}	$^1A_1$	−654.7527	125.46
Fig. 10g	$C_{10}N_5^-$	C_{2v}	$^1A_1$	−654.7257	142.46
Fig. 10h	$C_{10}N_5^-$	Cs	$^3A'$	−654.6833	169.02
Fig. 11a	$C_{11}N_5^-$	C_{2v}	$^1A_1$	−692.9761	0.00
Fig. 11b	$C_{11}N_5^-$	C_{2v}	$^3A_2$	−692.9709	3.26
Fig. 11c	$C_{11}N_5^-$	C_{2v}	$^1A_1$	−692.9261	31.37
Fig. 11d	$C_{11}N_5^-$	C_{2v}	$^3A_2$	−692.8832	58.31
Fig. 11e	$C_{11}N_5^-$	C_{2v}	$^1A_1$	−692.8427	83.71
Fig. 11f	$C_{11}N_5^-$	C_{2v}	$^3A_1$	−692.8225	96.38
Fig. 11g	$C_{11}N_5^-$	C_{2v}	$^3A_2$	−692.8022	109.12
Fig. 12a	$C_{12}N_5^-$	C_{2v}	$^1A_1$	−731.1181	0.00
Fig. 12b	$C_{12}N_5^-$	C_{2v}	$^1A_1$	−731.0688	30.94
Fig. 12c	$C_{12}N_5^-$	C_{2v}	$^1A_1$	−731.0277	56.73
Fig. 12d	$C_{12}N_5^-$	C_{2v}	$^1A_1$	−731.0219	60.37
Fig. 12e	$C_{12}N_5^-$	C_{2v}	$^1A_1$	−730.9956	76.87
Fig. 12f	$C_{12}N_5^-$	C_{2v}	$^1A_1$	−730.9708	92.43
Fig. 12g	$C_{12}N_5^-$	C_{2v}	$^3A_1$	−730.9595	99.52
Fig. 12h	$C_{12}N_5^-$	C_{2v}	$^1A_1$	−730.9537	103.16
Fig. 12i	$C_{12}N_5^-$	C_{2v}	$^1A_1$	−730.9206	123.93
Fig. 12j	$C_{12}N_5^-$	C_{2v}	$^3B_2$	−730.8905	142.82
Fig. 12k	$C_{12}N_5^-$	C_{2v}	$^1A_1$	−730.7065	258.28
Fig. 13a	$C_{13}N_5^-$	C_{2v}	$^3A_2$	−769.1564	0.00
Fig. 13b	$C_{13}N_5^-$	C_{2v}	$^1A_1$	−769.1402	10.17
Fig. 13c	$C_{13}N_5^-$	C_{2v}	$^1A_1$	−769.1350	13.43
Fig. 13d	$C_{13}N_5^-$	C_{2v}	$^3A_2$	−769.1010	34.76
Fig. 13e	$C_{13}N_5^-$	C_{2v}	$^1A_1$	−769.0937	39.34
Fig. 13f	$C_{13}N_5^-$	C_{2v}	$^1A_1$	−769.0427	71.35
Fig. 13g	$C_{13}N_5^-$	C_{2v}	$^3A_2$	−769.0318	78.35
Fig. 13h	$C_{13}N_5^-$	C_{2v}	$^3B_2$	−769.0089	92.56

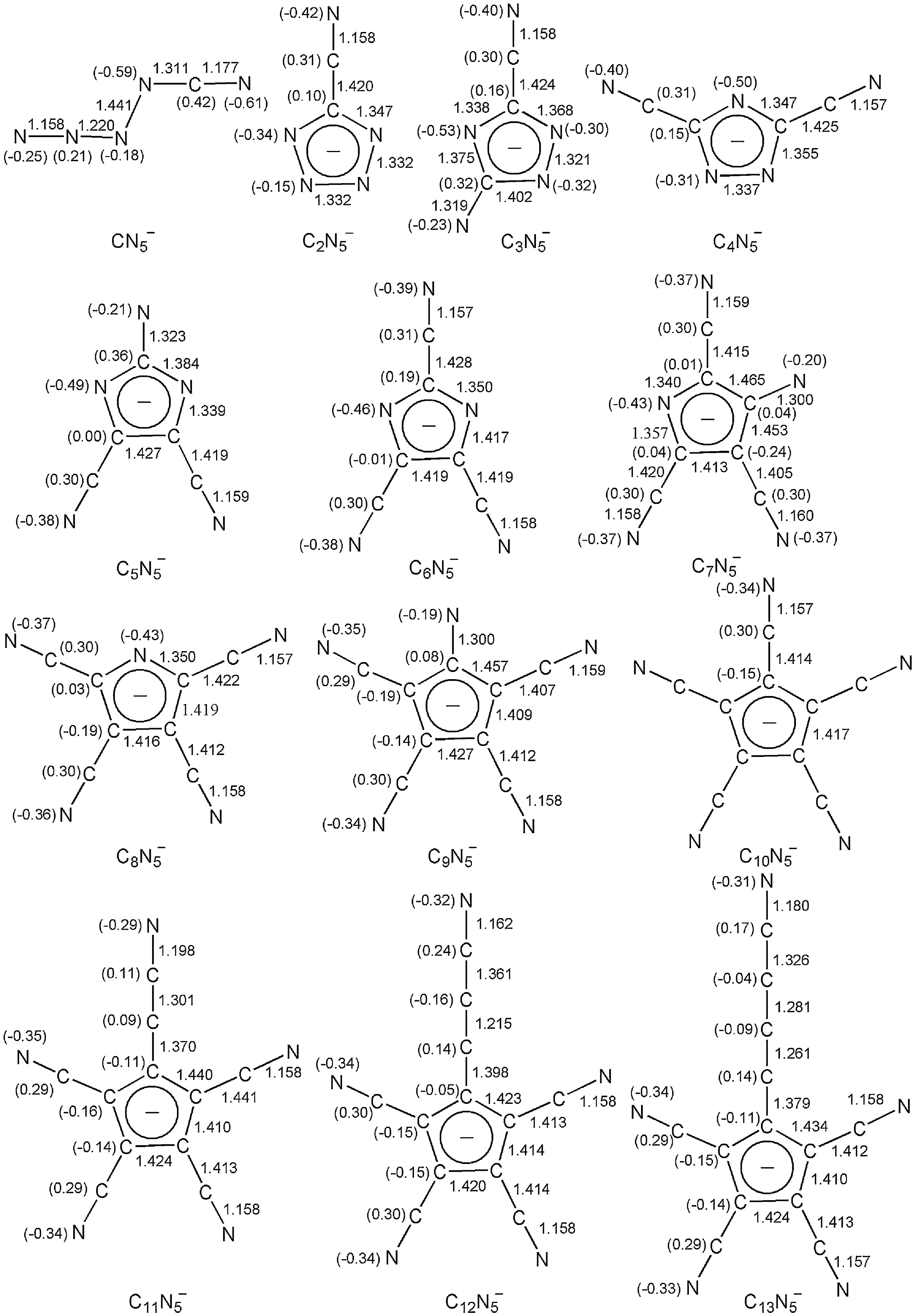

Fig. 14. Bond lengths (in Å) and NBO charges distributions (in parentheses) of the most stable $C_nN_5^-$ ($n = 1$–13).

with the nitrogen atoms within the pentagonal rings having "separated" nitrogen atom(s) are lower in energy. The isomers with "shared-edge" cyclic structures are generally high in energy, for example, those of Models 3i, 3j, 4i, 5e, 6j, 6k, 7j, 8k, 9i, 9j, 12j, 12k, 13g, and 13h.

Both nitrogen and phosphorus are Group VA elements; an atom of the two elements can offer five valence electrons for chemical bonding. Comparing C_nN^- [9] and $C_nN_2^-$ [17] to C_nP^- [29] and $C_nP_2^-$ [30,31], respectively, one can detect similarities in structure characteristics: (i) the locations of doped atom(s), (ii) the energies, and (iii) the odd/even alternate behaviors of the straight C_n chains. When the number of doped atoms is three, the binary clusters differ in geometry. The ground-state structures of $C_nP_3^-$ are straight carbon chains with a P_2C ring located at one end and a phosphorus atom at the other, and there is this alternate behavior of even-n clusters being more stable than odd-n clusters [32]. For the $C_nN_3^-$ ($n = 3$–8) clusters, the ground-state isomers show three branches, each with a nitrogen atom located at the end. When $n = 5$–8, the longest branch of $C_nN_3^-$ is polyacetylene-like. When $n = 5$ or 7, the longest branch is connected to the central sp^2 carbon in a non-linear fashion [19]. When the number of doped atoms is five, the binary clusters also show different geometric configurations. The ground-state structures of $C_nP_5^-$ ($n = 1$–7) are straight carbon chains with a P_4C ring located at one end and a phosphorus atom at the other [33].

3.2. Bonding characters

Depicted in Fig. 14 are the bond lengths and NBO charges of the most stable $C_nN_5^-$ ($n = 1$–13) structures. The C–N distance measured experimentally is 1.153 Å in hydrogen cyanide (prototypical C≡N triple bond), 1.209 Å in isocyanic acid (prototypical C=N double bond), and 1.376 Å in formamide (prototypical C–N single bond) [9,27]. As revealed in Fig. 14, with bond lengths within the 1.157–1.159 Å range, the C–N bonds of cyano groups bonded to carbon atoms of the pentagonal rings are triple bonds; the bond lengths of the exocyclic C–C bonds (within the 1.405–1.441 Å range) are between that of single and double C–C bonds. The N–N bonds of the pentagonal rings have bond lengths of 1.321–1.337 Å, intermediate to the generally accepted lengths of single (1.450 Å) and double (1.250 Å) N–N bonds of similar bonding environments. The bond lengths of C–N in the ring structures are in the range of 1.338–1.384 Å, that is between that of single and double C–N bond.

According to our NBO charge calculations, the atomic charge of any of the pentagonal rings in Fig. 14 varies from −0.58 to −0.88, and the rest of the negative charge of $C_nN_5^-$ is residing on the cyano group(s). In other words, the majority of the negative charge of the isomers is located within the rings. Tang et al. carried out B3LYP/6-31G* calculations on $C_{2n}N_5^-$ ($n = 1$–6) clusters and found that the atomic charges within the rings obtained from Mulliken population analysis vary from −0.74 to 0.38 [18]. It is apparent that the Mulliken population analysis using such basis set without diffuse function could result in unreasonable charge values within the rings of the $C_{2n}N_5^-$ ($n = 1$–6) anions.

For the ground-state isomers of $C_nN_5^-$ ($n = 2, 4, 6, 8$), both carbon and nitrogen atoms of the pentagonal rings are sp^2 hybridized and each nitrogen atom has a pair of dangling electrons. The p_z-orbital electrons of the atoms of the ring and the delocalized electron of the anion form a system of 6π electrons. In other words, there is a system of 6π electrons on a planar five-membered ring, analogous to that of the aromatic cyclopentadienyl anion. Furthermore, the triple bond of the cyano group(s) can conjugate with the π bond of the ring, resulting in better stability of the species. Lord et al. calculated electron affinities (EA) of pentacyanocyclopentadienyl by means of B3LYP, BLYP, and BP86 methods with DZP++ basis set. They interpreted that the large EA values are a result of stabilization induced by aromaticity, π-system delocalization, and the electron-withdrawing effect of the five cyano groups [20].

For $C_nN_5^-$ ($n = 3, 5, 7, 9$), the ground-state structures of bonding characters can be considered to be similar to those of $C_nN_5^-$ ($n = 4, 6, 8, 10$), respectively. The differences are one carbon atom in the five-membered ring is bonded to a nitrogen atom (not to a cyano group), and the C–N bond lengths are with length of 1.300–1.323 Å, characteristic of that between single and double bond. The p_z-electrons of the ring atoms and the delocalized electron of the anion form a system of 6π electrons, the cyclic structure with $4m + 2$ ($m = 1$) π electrons show aromatic character. The triple bond of the cyano group(s) and the nitrogen atom bonded to the ring can conjugate to the delocalized π bonding, resulting in a reduction in total energy.

In the straight NC_3– branch of ground-state $C_{12}N_5^-$, the terminal C–N bond length is 1.162 Å, displaying the characteristic of triple bond, and the C–C bond lengths show obvious short/long alternation, reflecting some sort of polyacetylenic-like character. As for the NC_2– and NC_4– branch of ground-state $C_{11}N_5^-$ (Model 11b) and $C_{13}N_5^-$ (Model 13a), respectively, the terminal C–N bonds with lengths of 1.180–1.198 Å and the C–C bonds of the chains tend to average out in length, exhibiting some sort of cumulenic-like character. In the hexagonal ring of Model 11a, the carbon atoms are sp^2 hybridized and the one without a cyano group shows a pair of dangling electrons. The p_z-orbital (perpendicular to the hexagonal plane) electrons of the ring and the delocalized electron of the anion form a system of 6π electrons, and the triple bonds of the five cyano groups conjugate with the π bond of the ring, and the electron-withdrawing effect of the five cyano groups, causing a reduction in total energy.

Shown in Fig. 15 are the schematic π molecular orbitals of 3D isosurface of ground-state $C_5N_5^-$ and $C_6N_5^-$. The p_z-orbitals of the atoms in the structures overlap to form delocalized π bonding, the cyano group and nitrogen atom bonded to the ring conjugate with the delocalized π bonding of the ring, resulting in a reduction in total energy. The other ground-state models of $C_nN_5^-$ display orbital of similar nature.

The electron states of ground-state $C_nN_5^-$ with odd and even number of carbon atoms are different; it is singlet for even n, and triplet for odd n. When n is odd, the number of alpha electrons in the triplet-state is larger than that of the beta electrons by 2, whereas when n is even, the numbers of alpha and beta electrons in the singlet state are the same. The effects of difference in parity suggest that the ground states with n even are more stable: it

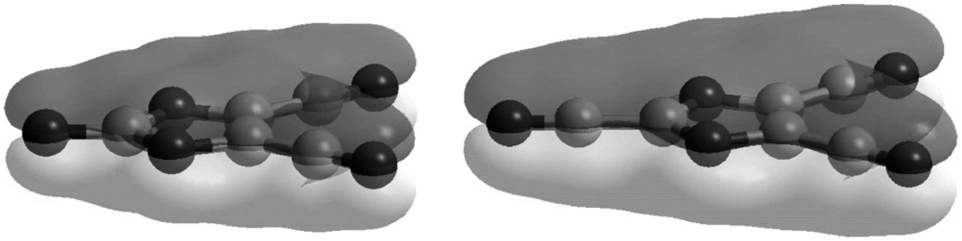

Fig. 15. Schematic diagrams of π molecular orbitals of 3D isosurface of ground-state $C_5N_5^-$ and $C_6N_5^-$.

requires more energy to remove an electron from a closed-shell configuration (n even) than that from an open-shell configuration (n odd).

3.3. Energy differences

Listed in Table 2 are the energy difference, electron affinity, atomization energy, and incremental binding energy with zero point energy correction for ground-state $C_nN_5^-$ ($n = 1–13$)**.** To evaluate the relative stability of the clusters of different sizes, the energy difference $\Delta E_n = (E(C_nN_5^-) - E(C_{n-1}N_5^-))$, which is defined as the difference between the total energies of the adjacent clusters, is calculated. Displayed in Fig. 16 is the variation of energy difference (ΔE_n) of the most stable $C_nN_5^-$ ($n = 1–13$) against the number of carbon atoms, i.e., ΔE_n is displayed as a function of n. According to the characteristic odd/even alteration, the clusters with even n are with ΔE_n lower than those of the adjacent clusters with odd n. The observations reiterate that the clusters with even n are more stable than those with odd n.

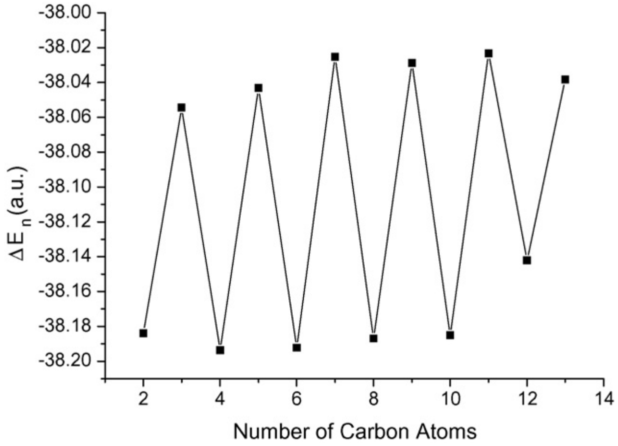

Fig. 16. Variation of energy differences ΔE_n (a.u.) of the most stable $C_nN_5^-$ ($n = 1–13$) clusters (as shown in Table 2) vs. number of carbon atoms.

3.4. Electron affinities

Electron affinity (EA, adiabatic) is computed as the energy difference between the optimized neutral and anionic (i.e., $E_{\text{neutral}} - E_{\text{anion}}$) clusters. A higher electron affinity means that more energy is released when an electron is added to a neutral molecule, and the production of the corresponding anion is more readily accomplished. The anionic cluster with a larger electron affinity is generally more stable. Electron affinity (EA) can be used as another means for the evaluation of the relative stability of anionic clusters with different sizes.

Fig. 17 depicts the EA values versus the number of carbon atoms in the most stable $C_nN_5^-$ ($n = 1–13$) clusters. There is a parity effect on the EA curve of $C_nN_5^-$: the *EA* of even-n clusters are in general higher than those of odd-n ones. This behavior reflects the higher stability of the even-n $C_nN_5^-$ clusters.

Table 2

Energy difference (ΔE_n) (a.u.), electron affinity (EA) (kcal/mol), atomization energy (ΔE_a) (a.u.), and incremental binding energy (ΔE^I) (a.u.) with zero point energy correction for the most stable $C_nN_5^-$ ($n = 1–13$)

Figure	Cluster	ΔE_n	EA	ΔE_a	ΔE^I
Fig. 1a	CN_5^-		63.38	0.9982	
Fig. 2a	$C_2N_5^-$	−38.1840	101.72	1.3249	0.3267
Fig. 3a	$C_3N_5^-$	−38.0544	83.08	1.5221	0.1972
Fig. 4a	$C_4N_5^-$	−38.1936	127.64	1.8584	0.3363
Fig. 5a	$C_5N_5^-$	−38.0433	87.10	2.0444	0.1860
Fig. 6a	$C_6N_5^-$	−38.1922	116.40	2.3794	0.3350
Fig. 7a	$C_7N_5^-$	−38.0253	94.69	2.5474	0.1680
Fig. 8a	$C_8N_5^-$	−38.1869	121.23	2.8770	0.3296
Fig. 9a	$C_9N_5^-$	−38.0289	98.33	3.0487	0.1717
Fig. 10a	$C_{10}N_5^-$	−38.1850	126.57	3.3764	0.3277
Fig. 11a	$C_{11}N_5^-$	−38.0234	106.78	3.5423	0.1659
Fig. 12a	$C_{12}N_5^-$	−38.1420	123.86	3.8270	0.2847
Fig. 13a	$C_{13}N_5^-$	−38.0383	105.50	4.0080	0.1810

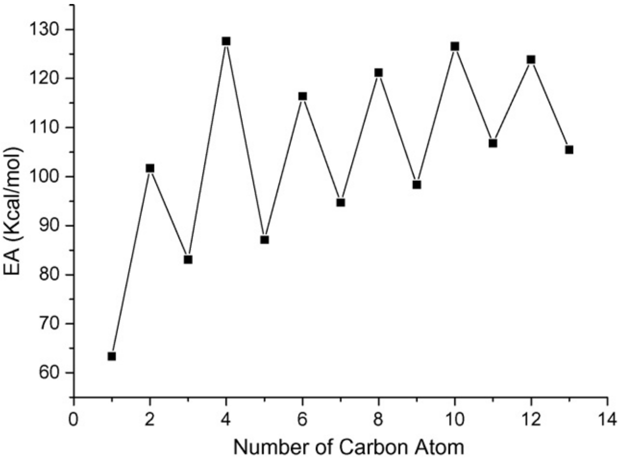

Fig. 17. Curve of electron affinity (EA) (kcal/mol) of the most stable $C_nN_5^-$ ($n = 1–13$) clusters (as shown in Table 2) vs. the number of carbon atoms.

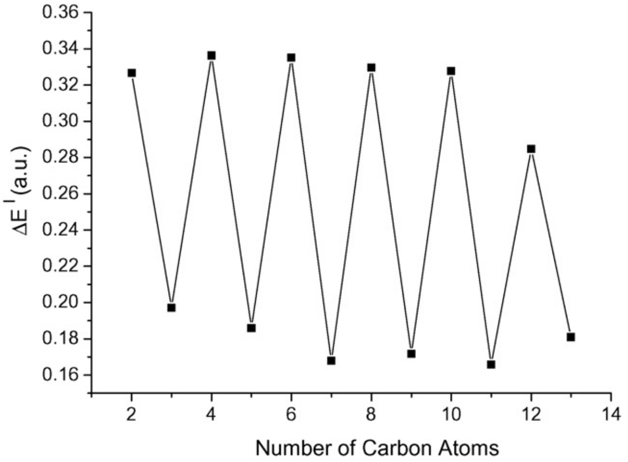

Fig. 18. Incremental binding energy ΔE^{I} (a.u.) of the most stable $C_nN_5^-$ ($n = 1$–13) clusters (as shown in Table 2) vs. the number of carbon atoms.

3.5. Incremental binding energies

The incremental binding energy (ΔE^{I}) which is the atomization energies (ΔE_{a}) difference of adjacent clusters can also reflect the relative stability of the anionic clusters (Table 2) [29]. We have

$$\Delta E^{\mathrm{I}} = \Delta E_{\mathrm{a}}(C_nN_5^-) - \Delta E_{\mathrm{a}}(C_{n-1}N_5^-)$$

where ΔE_{a} is defined as the energy difference between a molecule and its component atoms:

$$\Delta E_{\mathrm{a}} = nE(\mathrm{C}) + 5E(\mathrm{N}) - E(C_nN_5^-)$$

As showed in Fig. 18, the values of ΔE^{I} vary according to a pattern of odd/even alternation: when n is even, the ΔE_n value is large; when n is odd, the ΔE_n is small. Because a larger ΔE^{I} value implies a more stable $C_nN_5^-$ structure, one can deduce that a $C_nN_5^-$ ($n = 1$–13) cluster with even n is more stable than that with odd n.

Such odd–even alternate pattern of energy differences, electron affinities, and incremental binding energy is consistent with the experimental observation of Tang et al. [5]. The missing of odd-*n* peaks or products in experimental studies can be explained by a combined consideration of the overall behaviors of electron affinities (EA) and the incremental binding energies of the anionic clusters. Since the electron affinities and the incremental binding energies of the anionic clusters are obviously low when *n* is odd, compared to the even-*n* clusters, the odd-*n* ones are less stable and decompose more readily.

4. Conclusions

The ground-state structures of $C_nN_5^-$ ($n = 2$–13) contain a planar pentagonal ring of nitrogen and/or carbon atoms. When $1 < n \leq 10$, one carbon atom in the pentagon ring is bonded to a nitrogen atom when n is odd, when n is even, each carbon atom of the ring is bonded to a cyano group. With $n = 11$–13, a carbon atom of the pentagon is bonded to a straight carbon chain with a nitrogen atom located at the end, and the chain exhibits polyacetylene character when n is even, and cumulenic character when n is odd. The $C_nN_5^-$ ($n = 1$–13) with an even number of carbon atoms are more stable than those with odd numbers. The trend of odd/even alternation in stability can be explained according to the variation in bonding characters, energy differences, electron affinities, and incremental binding energies. The results of the calculation are in good agreement with the phenomena observed in experimental mass spectrometric studies.

Acknowledgment

The authors thank the National Science Foundation (Grants 20473061 and 20533020) for financial supports.

References

[1] M.B. Bell, P.A. Feldman, S. Kwok, H.E. Matthews, Nature 295 (1982) 389.
[2] K. Kawaguchi, S. Takano, M. Ohishi, S.I. Ishikawa, K. Miyazawa, N. Kaifu, K. Yamashita, S. Yamamoto, S. Saito, Y. Ohshima, Y. Endo, Astrophys. J. 396 (1992) L49.
[3] E. Herbst, Angew Chem. Int. Ed. Engl. 29 (1990) 595.
[4] C. Niu, Y.Z. Lu, C.M. Lieber, Science 261 (1993) 334.
[5] Z.C. Tang, R.B. Huang, L. Shi, L.S. Zheng, Int. J. Mass Spectrom. Ion Process. 173 (1998) 71.
[6] I. Zergioti, I. Alexandrou, A. Sfounis, G.A.J. Amaratunga, C. Fotakis, M. Velegrakis, Appl. Surf. Sci. 197–198 (2002) 387.
[7] C.R. Wang, R.B. Huang, Z.Y. Liu, L.S. Zheng, Chem. Phys. Lett. 237 (1995) 463.
[8] C.G. Zhan, S. Iwata, J. Chem. Phys. 104 (1996) 9058.
[9] G. Pascoli, H. Lavendy, Chem. Phys. Lett. 312 (1999) 333.
[10] J. Tittle, D. Merkoziaj, R. Liu, Chem. Phys. Lett. 305 (1999) 451.
[11] J. Armstrong, L. Degoricija, A. Hildebrand, J. Koehne, P.E. Fleming, Chem. Phys. Lett. 332 (2000) 591.
[12] K. Chuchev, J.J. BelBruno, J. Phys. Chem. A 106 (2002) 4240.
[13] K. Chuchev, J.J. BelBruno, J. Phys. Chem. A 107 (2003) 1887.
[14] K. Chuchev, J.J. BelBruno, J. Phys. Chem. A 107 (2003) 11217.
[15] J.J. BelBruno, Chem. Phys. Lett. 270 (1997) 99.
[16] J.J. BelBruno, Z.C. Tang, R. Smith, S. Hobday, Mol. Phys. 99 (2001) 957.
[17] Z.Y. Jiang, X.H. Xu, H.S. Wu, Z.H. Jin, Int. J. Mass Spectrom. 230 (2003) 33.
[18] Z.C. Tang, J.J. BelBruno, R.B. Huang, L.S. Zheng, J. Chem. Phys. 112 (2000) 9276.
[19] M.D. Chen, J.W. Liu, L. Dang, Q.E. Zhang, C.T. Au, J. Chem. Phys. 121 (2004) 11661.
[20] R.L. Lord, S.E. Wheeler, H.F. Schaefer, J. Phys. Chem. A 109 (2005) 10084.
[21] Hypercube Inc., Hyerchem. Reference Manual, Waterloo, Ont., Canada, 1996.
[22] M. James, C. Crabbe, J.R. Appleyard, C.R. Lay, Desktop Molecular Modeller, Oxford University Press, Walton Street, Oxford, Great Britain, 1994.
[23] M.J. Frisch, G.W. Trucks, H.B. Schlegel, G.E. Scuseria, M.A. Robb, J.R. Cheeseman, V.G. Zakrzewski, J.A. Montgomery Jr., R.E. Stratmann, J.C. Burant, S. Dapprich, J.M. Millam, A.D. Daniels, K.N. Kudin, M.C. Strain, O. Farkas, J. Tomasi, V. Barone, M. Cossi, R. Cammi, B. Mennucci, C. Pomelli, C. Adamo, S. Clifford, J. Ochterski, G.A. Petersson, P.Y. Ayala, Q. Cui, K. Morokuma, P. Salvador, J.J. Dannenberg, D.K. Malick, A.D. Rabuck, K. Raghavachari, J.B. Foresman, J. Cioslowski, J.V. Ortiz, A.G. Baboul, B.B. Stefanov, G. Liu, A. Liashenko, P. Piskorz, I. Komaromi, R. Gomperts, R.L. Martin, D.J. Fox, T. Keith, M.A. Al-Laham, C.Y. Peng, A. Nanayakkara, M. Challacombe, P.M.W. Gill, B. Johnson, W. Chen, M.W. Wong, J.L. Andres, C. Gonzalez, M. Head-Gordon, E.S. Replogle, J.A. Pople, Gaussian 98 (Revision A.11), Gaussian, Inc., Pittsburgh, PA, 2001.
[24] A.D. Becke, J. Chem. Phys. 98 (1993) 5648.

[25] C. Lee, W. Yang, R.G. Parr, Phys. Rev. B 37 (1988) 785.
[26] B. Miehlich, A. Savin, H. Stoll, H. Preuss, Chem. Phys. Lett. 157 (1988) 200.
[27] W.J. Hehre, L. Radom, P.v.R. Schleyer, J.A. Pople, Ab Initio Molecular Orbital Theory, Wiley–Interscience, New York, 1986.
[28] J.B. Foresman, Æ. Frisch, Exploring Chemistry with Electronic Structure Methods, Gaussian Inc., Pittsburgh, PA, 1996.
[29] G. Pascoli, H. Lavendy, J. Phys. Chem. A 103 (1999) 3518.
[30] K. Fisher, I. Dance, G. Willett, Eur. Mass Spectrom. 3 (1997) 331.
[31] R. Zeng, J.B. Liu, C.Y. Huang, Z. Gao, J. Chin. U 21 (2000) 581.
[32] M.D. Chen, L.S. Zheng, Q.E. Zhang, M.H. Liu, C.T. Au, J. Phys. Chem. A 107 (2003) 10111.
[33] M.D. Chen, H. Liang, M.H. Liu, Q.E. Zhang, C.T. Au, Int. J. Mass Spectrom. 232 (2004) 165.